Copy
RM E51I11

NACA RM E51I11

RESEARCH MEMORANDUM

INVESTIGATIONS OF AIR-COOLED TURBINE ROTORS FOR TURBOJET ENGINES

I - EXPERIMENTAL DISK TEMPERATURE DISTRIBUTION IN MODIFIED J33 SPLIT-DISK ROTOR AT SPEEDS UP TO 6000 RPM

By Wilson B. Schramm and Robert R. Ziemer

Lewis Flight Propulsion Laboratory
Cleveland, Ohio

NATIONAL ADVISORY COMMITTEE
FOR AERONAUTICS

WASHINGTON
January 9, 1952

NACA RM E51I11

NATIONAL ADVISORY COMMITTEE FOR AERONAUTICS

RESEARCH MEMORANDUM

INVESTIGATIONS OF AIR-COOLED TURBINE ROTORS FOR TURBOJET ENGINES

I - EXPERIMENTAL DISK TEMPERATURE DISTRIBUTION IN MODIFIED J33 SPLIT-DISK ROTOR AT SPEEDS UP TO 6000 RPM

By Wilson B. Schramm and Robert R. Ziemer

SUMMARY

An experimental investigation is being conducted at the Lewis laboratory to establish general principles for the design of noncritical turbine rotor configurations. This investigation includes evaluation of cooling effectiveness, structural stability, cooling-air flow distribution characteristics, and methods of supplying cooling air to the turbine rotor blades.

Prior to design of a noncritical rotor, a standard turbine rotor of a commerical turbojet engine was split in the plane of rotation and machined to provide a passage for distributing cooling air to the base of each blade. The rotor was fitted with nontwisted, hollow, air-cooled blades containing nine tubes in the coolant passage.

In the investigation reported herein, the modified turbine rotor operated successfully up to speeds of 6000 rpm with ratios of cooling-air to combustion-gas flow as low as 0.02. The disk temperatures observed at these conditions were below 450° F when cooling air at 100° F was used from the laboratory air system. The calculated disk temperatures based on the correlation method presented for rated engine conditions were well below 1000° F at a cooling-air flow ratio of 0.02, which is considered adequate for a noncritical rotor. An appreciable difference in temperature level existed between the forward and rear disks. This temperature difference probably introduced undesirable disk stress distributions as a result of the relative elongations of the two disks. This investigation was terminated at 6000 rpm so that slight changes in the engine configuration could be made to relieve this condition.

INTRODUCTION

An investigation is being conducted at the NACA Lewis laboratory to extend the application of turbine cooling to full-scale turbojet engines and thereby eliminate extensive use of critical materials in the turbine rotors. Although the effectiveness of air cooling as a means of controlling blade temperature distribution is demonstrated for various coolant passage configurations in references 1 to 6, other factors must be considered in design and application of air-cooled noncritical turbine rotors. The internal blade coolant passage configuration imposes limitations on the external aerodynamics of the rotor blade which may influence over-all engine performance. The unconventional configurations may also cause additional disk stress limitations. The coolant passages within the rotor must be designed to provide uniform distribution of the cooling air at the entrance to the blade base, and an effective coolant supply system is required between the compressor bleed and rotor inlet with suitable leakage seals at the point of introduction into the rotor. Development of rotor configurations which facilitate more conventional mass-production methods must also be considered if high component producibility is to be obtained.

Many supply arrangements and rotor configurations to direct cooling air to the blade bases have been considered. A commonly proposed system, which has been successfully applied to some extent in the turbojet engine, consists of a thin sheet metal shroud and impeller located on one face of the turbine disk, which provide an air passage out to the rim by having unsymmetrical transverse passages in the rim structure to the cooling-air openings in the blade base. Preliminary design studies indicated the desirability of a rotor configuration in which the centrifugal load of the blades is carried in a symmetrical rim and disk structure and the cooling air is introduced through a symmetrical passage directly under the blade base. It was anticipated that such a rotor could be cooled uniformly from its central plane, would be structurally stable, and would also effect a uniform chordwise distribution of cooling air within the blade shell. On the basis of these requirements, a split-disk rotor configuration was selected which had cooling air supplied through the tail cone to a central hole in the rear disk.

The principal uncertainty in design of rotors for air-cooled noncritical turbines is the lack of adequate data on disk temperature distribution over a range of blade cooling-air flows. In this investigation, the magnitude and behavior of internal temperature gradients in a disk and its operating temperature level at the cooling-air flows required for acceptable blade temperatures were sought prior to fabrication of a similar noncritical rotor. The computed stresses in a disk structure of the type used in this investigation, having a supply hole in the rear disk, and the results of a cold spin test of a similar rotor as well as the design of the supply duct in the tail cone that introduces the cooling air into the rotor are discussed in reference 7.

For this investigation, a standard J33 turbine disk of 16-25-6 alloy was altered to provide the desired configuration and fitted with 54 nontwisted air-cooled blades, cast of high-temperature alloy X-40 and containing nine tubes in the coolant passage. No attempt was made to correct the aerodynamic design of the blades for the initial rotor. An internal vane system was incorporated that was considered to be primarily a distributer rather than a compressor because the low circumferential speed at the tip of the vanes limited the pressure rise available even at high internal efficiencies.

The measured disk temperature distributions obtained from preliminary operation of the engine as well as disk temperatures predicted for rated sea-level static conditions are presented herein. The runs reported were conducted at engine speeds of 4000, 5000, and 6000 rpm, over a range of cooling-air flows from 2 to 10 percent of the combustion-gas flow. The initial phase of the investigation was terminated at 6000 rpm in order to correct a difference in temperature level encountered between the forward and rear disks by modifying the engine configuration.

SYMBOLS

The following symbols are used in this report:

h'	enthalpy based on total conditions (Btu/lb)
N	engine speed (rpm)
P	power (Btu/sec)
Q	heat gained (Btu/sec)
R	radius
T	temperature ($^{\circ}R$ or $^{\circ}F$)
w	weight flow (lb/sec)
Λ	temperature-recovery factor
φ	temperature-difference ratio $(T_{g,e} - T_D)/(T_{g,e} - T_{a,e,H})$

Subscripts:

a	cooling air
av	average

B	cooled blade
c	compressor
D	disk
e	effective
F	fuel
g	combustion gas
H	rotor hub
I	inlet
m	mixture of combustion gas and cooling air in tail pipe
S	stator
t	tail pipe
1 to 12	refers to disk thermocouple locations

APPARATUS

In this investigation of the cooling and structural problems encountered in an operating air-cooled turbine rotor, a J33 turbojet engine was utilized as a test facility. This engine had a dual-entry-type centrifugal compressor driven by a single-stage turbine and the combustion-chamber assembly consisted of 14 individual burners connected by flame propagation tubes.

Engine Modifications

Turbine modifications. - The design of the air-cooled turbine rotor is illustrated in figure 1. The standard turbine disk was split in the plane of rotation and each disk machined to provide a radial air passage from the point of introduction of the cooling air in the rear disk to the blade base; this operation reduced the total rotor thickness by 1/2 inch. The forward disk of the turbine was integral with the shaft and carried the torque. The rear disk formed one side of the air passage and permitted introduction of the cooling air through a central $3\frac{1}{4}$-inch diameter hole. An amount of metal corresponding to that removed in the air supply hole was removed from the center of the forward disk

as shown in figure 1 to equalize any radial elongations which might occur. The two disks were bolted together with eighteen 7/16-inch diameter body-fit bolts, with sufficient tension to adequately seal the parting line at the rim of the disks. An internal vane system, shown in figure 2, was milled integral with the disk halves. The 18 bolts that fastened the two disks together were buried within the impeller vanes and thus offered no obstruction to the cooling-air flow. The cooling-air flow path within the turbine rotor was designed to transfer as effectively as possible the cooling air from a plane perpendicular to the axis of the turbine to a plane through the axis under each blade.

The cooling-air supply tube, which was a part of the tail-cone assembly (figs. 3 and 4), was piloted in a labyrinth seal by a spider, shown in the right-hand view of figure 2. This spider was, in turn, piloted through sealed bearings (fig. 1) by the spindle which extended from the forward disk and the spindle and fairing formed the inner boundary of the cooling-air supply passage. The tips of the spider, which remained stationary, were concentric with the turbine shaft. Piloting of the cooling-air supply tube is essential because seal misalinement due to thermal distortions and loading of the tail-cone structure may result in excessive loss of cooling air.

Turbine blades. - The nontwisted air-cooled blades (fig. 5) used in the rotor were made with the same outside profile as blade 4 in reference 4, because the dies were available. The cooling-air passage of the blade was packed with nine tubes which ended at the platform of the blade base and thus the blade shell at the root section was forced to carry the entire weight of the tubes. Ending the tubes at the blade platform was necessary because the blade base was 1/2 inch shorter than the original because of the splitting of the disk. Therefore, the cooling-air passage within the blade base tapered from the blade profile (fig. 5(a)) at the top of the base to the profile shown in figure 5(b).

The blade shell and base were precision cast from the high-temperature alloy X-40. The cooling-air passage was of constant area from blade root to tip and the wall tapered linearly from the root to the tip. The nominal thickness of the wall was 0.030 inch at the tip and 0.060 inch at the root. The nine stainless steel tubes were inserted in the blade shell from the tip and brazed in place. The arrangement and size of these tubes are shown in figure 5(a).

Tail-cone modifications. - Although compressor bleed air for cooling is probably necessary in a flight installation, the laboratory high-pressure air system was used to supply the cooling air to the rotor in this investigation in order to hasten the operation of the turbine, to maintain better control, and to extend the range of operation. The standard engine tail cone was modified to provide introduction of the cooling air as shown in figures 3 and 4, and discussed in reference 7.

Instrumentation

Rotating thermocouple system. - The rotating blade and disk thermocouples were connected to the insulated terminals on the terminal ring (fig. 6), clamped along the face of the disk, and passed through a 3/8-inch radial hole in the shaft that provided access to the 3/8-inch axial hole in the shaft as shown in figure 3. Forty-eight 28-gage lead wires were run through the drilled turbine shaft and the compressor to a disconnect and indexing coupling and then to a slip-ring-type thermocouple pickup which is shown in figure 7. This disconnect and indexing coupling consisted of a commercial pin and socket connector fitted with chromel and alumel pins and sockets. The 48 lead wires were soldered to the engine side of this connector and 24 wires from the thermocouple pickup were soldered to the other side. The connector was designed so that by rotating half of the connector 180° with respect to the other half, either group of 12 thermocouples could be connected.

Blade instrumentation. - Three blades located approximately 120° apart, were each equipped with three blade wall thermocouples and one thermocouple that measured the cooling-air temperature in the blade root. These 12 thermocouples formed one group in the indexing coupling. Data on the blades with thermocouples are not reported herein.

Disk instrumentation. - The location of the disk thermocouples is shown in figure 8. Eight thermocouples were placed on the forward disk and were located so as to enable measurement of the radial temperature profile of the disk as well as the temperature gradient across the disk thickness. Thermocouples 1, 2, and 4 were placed about 0.14 inch beneath the outside surface of the disk. Thermocouples 3, 5, and 8 were placed about the same distance from the inner surface of the forward disk, thermocouples 3 and 5 being located under a cooling-air passage and thermocouple 8 under a vane, to determine if the part of the disk beneath the vane was cooled by the extended heat-transfer surface offered by the vane. Thermocouple 6 was located in the turbine rim at a radius that corresponded to the base of the serrations. Thermocouple 7 was placed so as to give an average measurement of the serration temperature. Only three thermocouples, 9, 10, and 11, were located on the rear disk because of the necessity of drilling a hole through the disks to bring the wires to the terminal ring on the front face (fig. 6). The installation of the thermocouples in the rear disk is shown in figure 9. These thermocouples were positioned approximately in the center of the disk width to give an average radial temperature profile of the rear disk. Thermocouple 12 was placed on the spindle directly beneath the inner race of the foremost spider bearing (fig. 8).

The assembly of the 36-gage chromel-alumel thermocouples was the same as that for the air-cooled blades described in reference 1. The

thermocouples were insulated inside 0.040-inch Inconel tubing and inserted in the holes drilled in the disk. The Inconel tubing, with the leads inside, was attached by spot-welded straps to the side of the disk as shown in figure 6 and the tubing terminated near the insulated bolts located on the thermocouple terminal ring.

Cooling-air supply control and instrumentation. - The cooling-air flow to the disk was measured by a standard ASME flat plate orifice and was controlled by remote-control valves. The cooling-air inlet temperature to the turbine rotor was measured by the two open-end iron-constantan temperature probes located on the survey rake in the cooling-air supply tube (fig. 4). Additional instrumentation in the tail cone consisted of two chromel-alumel thermocouples spot-welded to the surface of the baffle plate.

Engine instrumentation. - The turbine speed was regulated for any particular run by the use of a stroboscopic tachometer and a chronometric tachometer was used to measure the speed. The compressor inlet temperature was measured by three shielded thermocouples on both the front and rear inlets, which were spaced equally about the circumference. The compressor outlet temperature and total and static pressures were measured by probes located in the diffuser section just downstream of the compressor. The engine mass flow was calculated from temperature and total and static pressure readings obtained from a survey rake located in the tail pipe approximately 6 feet downstream of the turbine. Fuel flow was measured by means of a calibrated rotameter.

EXPERIMENTAL PROCEDURE

The turbine was operated at various speeds and cooling-air flows. For a given speed, which was regulated by the use of a stroboscopic tachometer, the cooling-air flow was varied by means of the remote-control valves. For all runs reported herein the adjustable exhaust nozzle was maintained in the full-open position ($20\frac{13}{16}$-inch diam.). The 12 thermocouples in the disk were arranged in the disconnect and indexing coupling so that indexing was not necessary to obtain readings on all disk thermocouples. Engine starting and operating procedures were standard. When the engine was shut down, however, the cooling-air flow was maintained after the fuel was shut off in an effort to cool the disk so that the bearings on the spindle shaft would not be heated by the large heat source in the disk.

The data presented herein were obtained at three engine speeds, 4000, 5000, and 6000 rpm. A summary of the engine operating conditions is given in table I. For each speed the cooling-air flow was varied from 10 percent to approximately 2 percent of the compressor mass flow.

CALCULATION PROCEDURE

Correlation of Disk Temperatures

At present, no analytical method is known for predicting air-cooled disk temperatures such as the method developed in reference 8 and used in reference 1 to predict the spanwise temperature distribution of an air-cooled blade. A method has been started, however, by considering a differential section of the disk and expressing the heat-balance equations for this section on the basis of the conduction and convection processes. The preliminary equation for predicting disk temperatures is of third-order differential form and is a function of the geometric location and size of the element under consideration, the heat-transfer coefficient on the outside of the disk, the heat-transfer coefficient on the cooling-air side of the disk, the conductivity of the material, the effective gas temperature, the effective cooling-air temperature at the cooling-air inlet, the cooling-air weight flow, and the disk speed. In equation (1) of reference 1 the blade temperature is a function of the same general terms mentioned for the disk temperature with the exception that the thermal conductivity has been neglected in the blade-temperature equation. Because of the functional similarity between the two equations, a temperature difference ratio that describes the effectiveness of the cooling process and is similar to that used in reference 1 should correlate the disk temperatures, at least for a given turbine speed.

Since some of the observed disk temperatures are rather low, values of the temperature-difference ratio $\varphi = \frac{T_{g,e} - T_D}{T_{g,e} - T_{a,e,H}}$ (equation (1), reference 1) near 1.0 would be obtained. Thus, small variations in the values of T_D would affect the percentage change of this ratio very little. For this reason, the disk temperature data have been correlated on the basis of $(1 - \varphi) = \frac{T_D - T_{a,e,H}}{T_{g,e} - T_{a,e,H}}$ where small variation of T_D will affect the temperature-difference ratio markedly.

Determination of Turbine Inlet Temperatures

Temperature and pressure measurements were not made at the stator inlet. Since the circumferential and radial temperature patterns from the burners varied widely, a large number of instruments would have been needed to obtain an accurate average. Therefore, it was necessary to calculate the average stator inlet temperature from the measurements of

the combustion gas and cooling-air mixture taken in the tail pipe downstream of the turbine. The static and total temperatures at this station were evaluated as in equations (15) and (16) of reference 1. The stator inlet conditions, based on the measurements made in the tail pipe, were determined by use of the energy equation which is based on the change in state of the combustion gas and the cooling air through the turbine. All the heat lost by the combustion gases in the tail cone was assumed to be gained by the cooling air as it passed through the tail cone. This energy equation, which was developed in reference 9, is as follows:

$$(w_g h'_{g,S,I} - P_c - P_a - Q_{a,B}) + (w_a h'_{a,I} + P_a + Q_{a,B} + Q_{a,t}) - Q_{a,t} = w_m h'_m \quad (1)$$

where

$h'_{a,I}$ total enthalpy of blade cooling air outside tail cone (Btu/lb)

$h'_{g,S,I}$ total enthalpy of combustion gases at stator inlet (Btu/lb)

h'_m total enthalpy of mixture of combustion gases and cooling air in tail pipe (Btu/lb)

P_a power to pump blade cooling air (Btu/sec)

P_c power required by compressor (Btu/sec)

$Q_{a,B}$ heat gained by cooling air passing through cooled blades (Btu/sec)

$Q_{a,t}$ heat gained by cooling air passing through tail cone (Btu/sec)

w_a cooling-air weight flow (lb/sec)

w_g combustion-gas weight flow (lb/sec)

w_m weight flow of mixture of combustion gas and cooling air in tail pipe (lb/sec)

The average total temperature of the combustion gas at the stator inlet was evaluated in a manner similar to that described in reference 1. Equation (1) is based on the assumption that the mixture of combustion gases and cooling air downstream of the turbine is complete and that the rake in the tail pipe measures a true mixture temperature. In reference 1 only two of the 54 blades were cooled and the net effect of the cooling air, scavange air, and bearing air on the measurements taken in

the tail pipe was somewhat less than on the configuration considered herein. If the cooling air discharging from the tips of the blades does not mix thoroughly with the combustion gases but instead flows along the outer wall of the tail cone, the temperatures measured by the rake may not be the true average mixture temperature even though the rake extends entirely across the tail pipe. However, the calculated effective gas temperatures are estimated to be accurate to within 4 percent of the true effective gas temperature. The methods of determining the stator inlet pressures and the thermodynamic properties of the combustion gas and the cooling air are the same as those described in reference 1.

Determination of Effective Gas Temperature

In order to calculate the values of $1 - \varphi$ for use in the correlation procedure, or to determine the disk temperatures when the values of $1 - \varphi$ are known, the effective gas temperature $T_{g,e}$ at the rotor blade must be evaluated. The interrelation of the effective gas temperature and the total and static gas temperatures and the temperature recovery factor A is discussed in reference 1 and excellent correlation with the measured effective gas temperature over the range of temperatures investigated is shown. The recovery factor used for the calculations described herein was determined in the same manner as that described in reference 1.

No measurements were made in the combustion-gas stream between the stator blades and the rotor blades, because the space available was small and many surveys would have been required to obtain an accurate average of temperatures and pressures. The calculation procedures for determining the total and static temperatures and pressures at the rotor blade inlet from the conditions at the stator blade inlet are explained in reference 1.

Cooling-Air Temperatures

The indicated cooling-air temperatures measured by the rake in the cooling-air supply tube were corrected to total temperatures for use in the evaluation of $h'_{a,I}$ in equation (1) in a manner similar to that described in reference 1. The indicated cooling-air temperature was used as the effective cooling-air temperature at the rotor inlet for correlation purposes. This simplification was based on the following assumptions: The temperature recovery factory of the thermocouple and of the disk were roughly of the same magnitude, the relative velocity at the entrance to the disk and the absolute velocity at the measuring station in the cooling-air supply tube were approximately the same, and little heat was transferred to the cooling air between the measuring station in the supply tube (fig. 4) and the entrance to the rotor. These assumptions should lead to little error in the temperature-difference ratio.

RESULTS AND DISCUSSION

The results of the experimental investigations on disk temperature measurements of the split-type air-cooled turbine rotor are presented in figures 10 through 15.

Experimental Data

Variation of disk temperatures and inlet cooling-air temperature with cooling-air flow. - The experimental data for several typical disk thermocouples and the cooling-air temperature at the inlet to the rotor are presented in figures 10, 11, and 12 for 4000, 5000, and 6000 rpm, respectively. The engine operating conditions for the points shown in figures 10 through 12 are presented in table I. The general trends of the observed disk and cooling-air temperatures are the same as that of the blade temperatures reported in reference 1. The temperatures measured in the forward disk, with the exception of that indicated by thermocouple 1, increased as the radial position increased, as would be expected. The apparent reason for the temperature indicated by thermocouple 1 being higher than or equal to that indicated by thermocouple 2 is that thermocouple 1 was shielded to some extent by the thermocouple terminal ring (fig. 6) and received no direct cooling from the external cooling air on the upstream face of the forward disk. In figure 10, thermocouple 11 in the rear disk (2.82-in. rad) is shown to have indicated a temperature level between that shown for thermocouples 4 and 6 (6.81- and 8.14-in. rad, respectively) in the forward disk. This condition is accentuated in figures 11 and 12 for 5000 and 6000 rpm, respectively. The temperature at position 11 in the rear disk at 5000 rpm rose higher than that of thermocouple 6 in the forward disk at a cooling-air flow of about 1.85 pounds per second. At 6000 rpm, this crossover occurred at 2.75 pounds per second and at the extremely low cooling-air flows of 0.70 pound per second the temperature in the rear disk at this inner radius reached a value almost equal to that indicated in the serrations in the forward disk. The temperature indicated by thermocouple 11 was also higher than that indicated by thermocouple 10 at the low cooling-air flows (fig. 12).

Disk temperature profiles at 6000 rpm. - Typical radial temperature profiles for two cooling-air flows for the forward and rear disk are shown in figure 13. The temperature profile of the forward disk was at a very low level and essentially flat from the innermost thermocouple location out to a radius of approximately $6\frac{1}{2}$ inches (fig. 13(a)). From this point out to the temperature measurement in the serrations, the temperature increased rapidly over the entire range of cooling-air flows, but even at the lowest cooling-air flow the serration temperature was 600° F lower than the effective gas temperature, which indicated effective cooling. The axial temperature gradient across the forward disk was negligible (see table II).

In figure 13(b), which presents the temperature profiles in the rear disk for the same conditions that are shown in figure 13(a), the temperature level out to a radius of 7.0 inches was considerably higher than that obtained for the forward disk. At the lower cooling-air flows, a reversal in the profile occurred, that is, thermocouple 11 read higher than thermocouple 10.

Correlation of disk temperatures. - By use of the parameter $1 - \varphi$ and the cooling-air flow ratio w_a/w_g, the correlation plots of the 11 thermocouples located in the disks are presented in figure 14. The temperatures obtained for each speed in the rear disk and in the forward disk near the rim showed good correlation and reproducibility when plotted on semilog coordinates. The data for the 4000 and 5000 rpm runs also correlated closely, but at 6000 rpm the correlation curve tends to be slightly lower which indicates better cooling than at the two previous speeds. The resulting plots in figures 14(d) to 14(j) indicate a straight line relationship. The data points for thermocouple 11, figure 14 (k), however, were correlated by a slightly curved line. When examining the behavior of this thermocouple in figures 10, 11, 12, and 13(b), it was thought that this point was affected by other factors that were not described by the temperature-difference ratio, possibly by radiation from the tail-cone baffle plate. The slight scatter of the correlation plots in figures 14(a), 14(b), and 14(c) appeared where the disk temperatures were in the 100° F range and the variation of temperature for a given speed over the range of cooling-air flows was small. The correlation relationship expressed in figure 14 merely indicated that for the three speeds investigated and for a specific cooling-air flow ratio, the ratio of gas-side to cooling-air side heat-transfer coefficients remained approximately constant. However, as previously mentioned, the 6000 rpm curve is slightly lower and as the speed is increased further shifts of the curves can probably be expected.

Temperature Distribution and Heat-Transfer Characteristics

The general temperature level of the two disks was very low, partly because of the direct cooling from the internal air flow, and partly because of the reduced heat transfer into the rim of the turbine. The temperature in the rear disk at any radial position was much higher than that in the forward disk. This temperature difference is thought to be caused by several factors. The forward disk was cooled externally as well as internally. In the normal engine installation, as was used in these investigations, ram air is supplied to the upstream face of the turbine and flows radially along the face of the wheel. Evidence of this severe cooling is shown in figure 13(a) which indicates that the temperature profile over the range of coolant flows investigated at 6000 rpm was about 100° F out to a radius of 6.0 inches. The causes of the high temperature level of the rear disk were thought to be radiation

from the tail-cone baffle plate (fig. 3), convection heating from the combustion gases in the chamber between the rear disk and the baffle plate, and possibly separation of the cooling air from the inner surface of the rear disk as the air turned radially outward from the supply tube into the impeller.

The primary reason for the two disks remaining at their respective temperature levels during operation was the insulating layer of air between them. In the normal operation of the solid disk, cooling of the upstream face and heating of the downstream face take place, but the temperatures tend to equalize somewhat by transverse conduction within the disk. This conduction process cannot take place to any great extent in the split-type disk.

As would be expected for cooling air on both sides of the forward disk, no appreciable transverse temperature gradient existed at the two radial positions investigated (see table II). Also, no difference appeared between the measurements obtained from thermocouples 5 and 8. This indicated that the extended heat-transfer surface offered by the impeller vanes did not affect the disk temperature directly beneath the vanes.

The extreme radial temperature gradient that was measured in the forward disk near the rim (fig. 13(a)) and the smaller gradient thought to exist in the rear disk were due to the fact that one of the primary heat sources was through the rim. The heat supplied by conduction from the blades into the disks and by direct convection heating by the combustion gases was approximately 5 percent of that transferred to the blades.

The temperature of the tail-cone baffle plate, measured by two thermocouples (fig. 4), indicated that it operated from 200° to 400° F hotter than the rear disk. The temperature of the baffle plate at the outer radius decreased as the cooling-air flow decreased. The measurements at the inner radius, while they follow the same general trend as the outer radius, were erratic, especially at the higher cooling-air flows. This unsteadiness may have been caused by cooling-air leakage past the labyrinth seals onto the baffle plate at the higher flows and pressures. This leakage might also explain the behavior of the temperatures measured at the inner radius of the rear disk (thermocouple 11) as presented in figures 10, 11, 12, and 13(b). At the higher cooling-air flows, and consequently greater leakage through the seal, any radiation from the baffle plate to the rear disk was reduced since the baffle plate was cooled by convection in this inner region. As the leakage was decreased at the lower cooling-air flows, radiation to the rear disk had more effect and the temperature at this point in the rear disk increased more rapidly than any of the other disk temperatures.

The temperatures of the spider bearing spindle for 4000 and 6000 rpm are plotted in figure 15 as a function of the cooling-air flow. Little effect of speed on these temperatures is indicated in this plot. The bearing temperature closely follows the inlet cooling-air temperature and operational difficulties could occur with commercially available bearings at high cooling-air inlet temperatures.

Estimated Disk Temperatures at Rated Engine Conditions

The correlation presented in figure 14 permits estimation of the disk temperature distribution at other operating conditions. Figure 16 shows such an estimation for the rated operating conditions of this engine at a speed of 11,500 rpm using 2 percent of the engine mass flow for cooling. These estimations were based on the data presented in figure 14 for 6000 rpm. If the correlation curves continue to shift downward, as indicated by the difference between the 4000 and 6000 rpm data, these estimates may be somewhat conservative. The calculated disk temperatures for a inlet cooling-air temperature of 120° F which would be obtained by cooling the bleed air between the compressor discharge and the inlet to the tail cone are presented in figure 16(a). The calculated points for a cooling-air inlet temperature of 445° F, which is slightly above compressor discharge temperature are shown in figure 16(a). The most significant observation to be derived from these calculated profiles is that the general temperature level of the turbine for the low blade cooling-air flow ratio of 0.02 specified was well below 1000° F even for the case of the high cooling-air inlet temperature used in figure 16(b). This level is believed to be sufficient for application of air-cooled noncritical disks. Other factors such as creep and corrosion resistance must be considered before a practical application can be made.

A marked temperature difference between the forward and rear disks is shown in figure 16. This temperature-level difference results in a differential thermal expansion which may influence the disk stress distribution considerably; detailed analysis of the effects on the stress distribution is discussed in reference 7. Reducing the cooling-air inlet temperature has a beneficial effect on the calculated temperature levels of the disks for the two cases presented in figure 16. Two modifications can be made to the existing engine configuration which might alleviate the difference in temperature level between the two disks. The most obvious modification is to restrict the flow of external cooling air over the forward disk. Care must be taken, however, that the rear turbine bearing does not overheat as this air helps to cool the bearing. The other modification that may be considered is to cool the rear disk by circulating cooling air inside the bullet of the tail cone, thus reducing the baffle plate temperature and reducing the radiation to the rear disk.

CONCLUDING REMARKS

The results obtained show that large reductions in disk temperature can be obtained with cooling-air flows required for acceptable blade temperature, and that the use of noncritical metals in the turbine disk appears feasible. Since the turbine rotor contains a large percentage of the critical alloys in the engine, substitution of a noncritical turbine disk will increase the number of engines that can be produced from a given amount of alloying elements. The alternative method of achieving a reduction in critical materials in the turbine and a corresponding increase in number of engines produced is to operate the engine at a lower temperature level, which may produce a marked loss in aircraft performance. Analyses conducted at the Lewis laboratory indicate, however, that air-cooling of the blades and disks can be achieved without excessive loss in aircraft performance. In addition, the use of low alloy materials greatly increases the variety of metal-forming processes available for producing disks and blades. It also appears from design studies that have been made, that the use of sheet metal components in the fabrication of the disks and blades is desirable if a high rate of production is to be obtained.

SUMMARY OF RESULTS

An investigation was conducted to evaluate the structural and cooling characteristics of an air-cooled split-disk turbine rotor configuration prior to design and fabrication of a similar noncritical rotor. A standard J33 disk of 16-25-6 alloy was modified for the investigation and fitted with cast X-40 alloy nine-tube air-cooled blades. The results of this investigation, which was conducted in a production turbojet engine, are summarized as follows:

1. The experimental air-cooled rotor was operated successfully at cooling-air flow ratios of 0.02 to 0.10 up to engine speeds of 6000 rpm.

2. Operation of the split-disk rotor indicates that good disk cooling can be obtained at the cooling-air flow ratios required for air-cooled noncritical turbine blades.

3. The observed temperature level of the two disks was below 450° F at an engine speed of 6000 rpm and cooling-air flow ratio of 0.02.

4. A considerable difference in temperature level of the two disks was encountered over the range of engine speed and cooling-air flow ratio investigated, which probably resulted from excessive cooling of the forward disk of the rotor. Because of the possibility that undesirable stress distributions in the two disks would result from the

difference in temperature level, the investigation was terminated at 6000 rpm so that slight modifications of the configuration could be made to relieve this condition.

5. Based on the correlation methods used, the calculated temperature level of the disks at rated engine conditions with low cooling-air flow ratio is well below 1000° F, which is believed sufficient for application of experimental air-cooled noncritical rotors.

Lewis Flight Propulsion Laboratory
National Advisory Committee for Aeronautics
Cleveland, Ohio.

REFERENCES

1. Ellerbrock, Herman H., Jr., and Stepka, Francis S.: Experimental Investigation of Air-Cooled Turbine Blades in Turbojet Engine. I - Rotor Blades with 10 Tubes in Cooling-Air Passages. NACA RM E50I04, 1950.

2. Hickel, Robert O., and Ellerbrock, Herman H., Jr.: Experimental Investigation of Air-Cooled Turbine Blades in Turbojet Engine. II - Rotor Blades with 15 Fins in Cooling-Air Passages. NACA RM E50I14, 1950.

3. Hickel, Robert O., and Smith, Gordon T.: Experimental Investigation of Air-Cooled Turbine Blades in Turbojet Engine. III - Rotor Blades with 34 Steel Tubes in Cooling-Air Passages. NACA RM E50J06, 1950.

4. Ellerbrock, Herman H., Jr., Zalabak, Charles F., and Smith, Gordon T.: Experimental Investigation of Air-Cooled Turbine Blades in Turbojet Engine. IV - Effects of Special Leading- and Trailing-Edge Modifications on Blade Temperature. NACA RM E51A19, 1951.

5. Smith, Gordon T., and Hickel, Robert O.: Experimental Investigation of Air-Cooled Turbine Blades in Turbojet Engine. V - Rotor Blades with Split Trailing Edges. NACA RM E51A22, 1951.

6. Arne, Vernon L., and Esgar, Jack B.: Experimental Investigation of Air-Cooled Turbine Blades in Turbojet Engine. VI - Conduction and Film Cooling of Leading and Trailing Edges of Rotor Blades. NACA RM E51C29, 1951.

7. Kemp, Richard, H., and Moseson, Merland L.: Investigations of Air-Cooled Turbine Rotors for Turbojet Engines. II - Mechanical Designs, Stress Analysis, and Burst Test of Modified J33 Split-Disk Rotor. NACA RM E51J03, 1952.

8. Livingood, John N. B., and Brown, W., Byron: Analysis of Spanwise Temperature Distribution in Three Types of Air-Cooled Turbine Blade. NACA Report 994, 1950. (Formerly RM E7B11e and RM E7G30.)

9. Ellerbrock, Herman H., Jr., and Ziemer, Robert R.: Preliminary Analysis of Problem of Determining Experimental Performance of Air-Cooled Turbine. III - Methods for Determining Power and Efficiency. NACA RM E50E18, 1950.

TABLE I - SUMMARY OF ENGINE OPERATING CONDITIONS

Series	Run	Engine speed N (rpm)	Average compressor-inlet condition		Average fuel flow w_f (lb/sec)	Combustion-gas flow w_g (lb/sec)	Cooling-air flow w_a (lb/sec)	Cooling-air flow ratio w_a/w_g	Cooling-air inlet temperature $T_{a,H}$ (°F)	Calculated effective gas temperature $T_{g,e}$ (°F)
			Total pressure (in. Hg absolute)	Temperature (°F)						
I	1	3998	29.48	47.3	0.355	21.00	1.622	0.077	61.5	1152
	2	3976	↓	↓	↓	20.99	1.479	.070	63.0	1145
	3	3998				20.74	1.969	.095	55.5	1174
	4	4030				21.05	1.848	.088	57.0	1168
	5	3998				20.83	1.778	.085	58.0	1169
	6	4000				21.06	1.350	.064	65.5	1150
	7	3998				21.16	1.244	.059	67.5	1146
	8	3994				21.16	1.131	.054	70.5	1143
	9	4004				21.59	.968	.045	75.0	1137
	10	4004				21.71	.718	.033	86.5	1135
II	11	4986	29.03	65.0	0.429	24.98	2.569	0.103	60.0	1205
	12	5040	↓	↓	↓	25.55	2.388	.093	59.0	1193
	13	4982				25.37	2.235	.088	60.0	1190
	14	4988				25.59	2.046	.080	62.5	1180
	15	5020				25.79	1.807	.070	66.5	1171
	16	5004				25.88	1.609	.062	70.5	1163
	17	4988				25.78	1.411	.055	75.5	1155
	18	4999				26.09	1.226	.047	79.5	1151
	19	4980				26.23	1.000	.038	88.5	1145
	20	4990				26.26	.706	.027	106.0	1144
III	21	5980	29.25	40.0	0.500	32.38	3.192	0.099	43.0	1056
	22	6002	↓	↓	↓	33.14	2.862	.086	45.0	1051
	23	5990				32.97	2.606	.079	46.5	1048
	24	6016					2.355		49.5	
	25	5997				33.06	2.072	.063	53.0	1032
	26	5988				33.92	1.802	.053	56.5	1036
	27	5996				33.84	1.573	.046	60.0	1036
	28	6024				34.47	1.283	.037	67.5	1035
	29	5998				33.97	1.010	.030	71.5	1030
	30	6018	↓	↓	↓	33.86	.701	.021	85.5	1024

TABLE II - SUMMARY OF MEASURED DISK TEMPERATURES

Series	Run	$T_{D,1}$ (°F)	$T_{D,2}$ (°F)	$T_{D,3}$ (°F)	$T_{D,4}$ (°F)	$T_{D,5}$ (°F)	$T_{D,6}$ (°F)	$T_{D,7}$ (°F)	$T_{D,8}$ (°F)	$T_{D,9}$ (°F)	$T_{D,10}$ (°F)	$T_{D,11}$ (°F)	Spindle T_{12} (°F)
I	1	98	93	92	122	112	183	303	111	262	186	167	100
	2	99	93	92	123	115	192	315	113	279	198	177	110
	3	98	89	85	113	101	165	277	102	226	165	147	102
	4	101	92	87	117	106		287	105	238	173	156	110
	5	100	92	88	118	107	182	292	107	244	177	158	110
	6	102	97	94	127	118	202	328	119	296	210	188	118
	7	102	100	98	133	123	210	342	125	313	224	200	118
	8	103	102	102	137	132	222	353	132	333	238		120
	9	103	102	104	144	138	250	374	137	363	265		120
	10	102	110	114	162	158		423	157	428	343		125
II	11	107	100	87	117	106	163	275	104	213	157	138	
	12	108	100	91	122	108	168	283	110	230	172	151	
	13	110	102	92	123	112	173	291	112	241	180	159	
	14	112	103	94	127	117	182	302	114	258	193	174	
	15	113	106	97	132	122	192	317	122	284	213	193	
	16	114	109	105	137	128	203	333	128	310	233	213	
	17	117	113	109	144	137	219	353	137	344	259	239	
	18	117	117	117	153	147	235	374	145	378	288	271	
	19	120	121	121	162	158	258	404	158	419	327	305	
	20	126	131	138	186	186	302	462	186	484	395		
III	21	87	81	73	99	86	132	232	86	200	150	128	74
	22	87	82	75	100	91	138	238	89	214	159	135	77
	23	90	83	78	103	93	145	248	93	228	170	142	80
	24	91	85	82	111	97	152	257	96	243	181	154	83
	25	91	87	84	112	102	159	272	101	263	194	168	85
	26	92	90	87	118	110	171	287	110	287	213	185	93
	27	93	91	89	117	112	180	299	112	304	230	202	94
	28	100	95	96	129	123	197	326	122	343	261	242	107
	29	101	100	105	138	134	221	354	133	377	302	321	110
	30	107	108	115	154	153	252	393	153	420	353	387	122

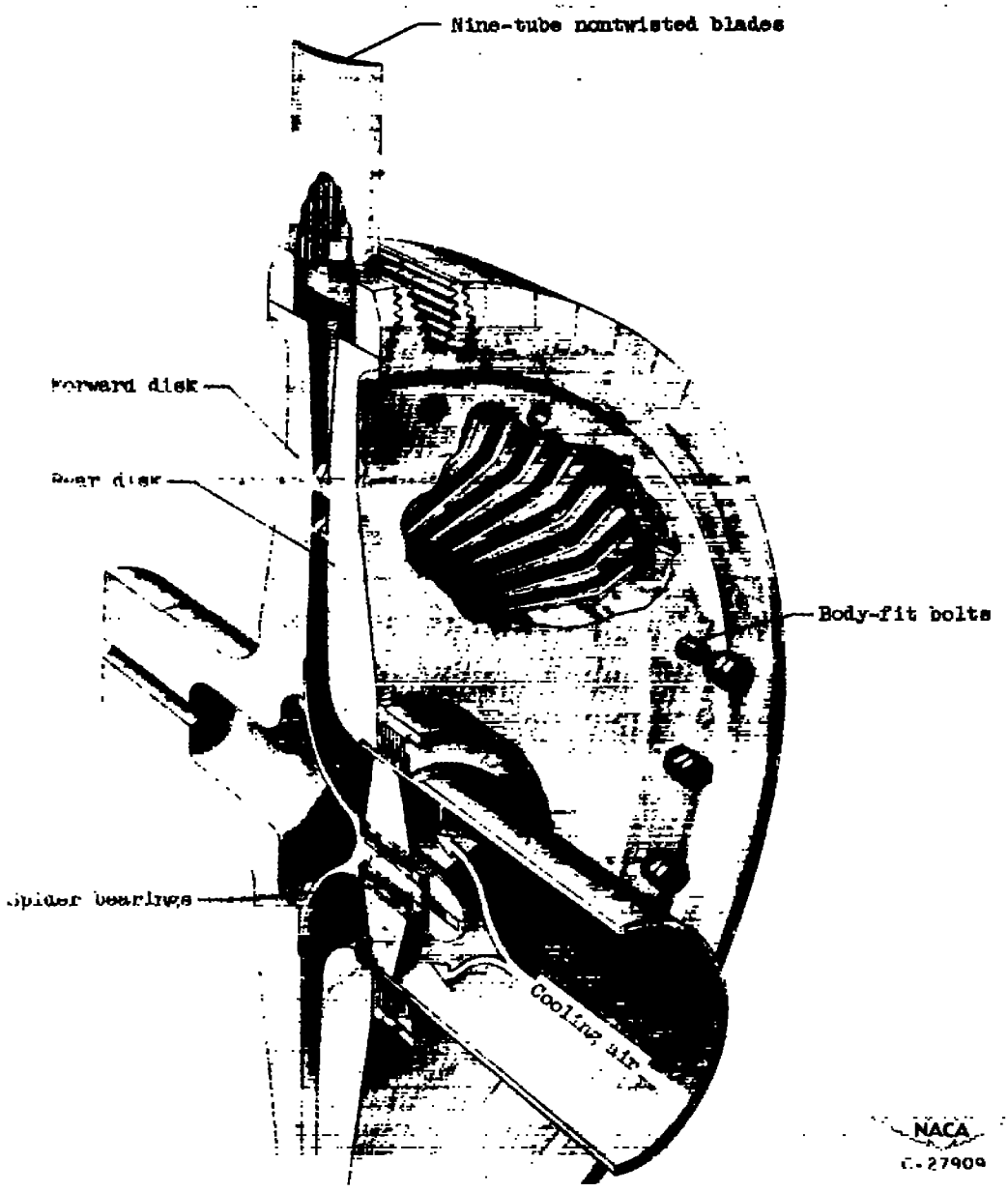

Figure 1. - Modified J33 air-cooled turbine.

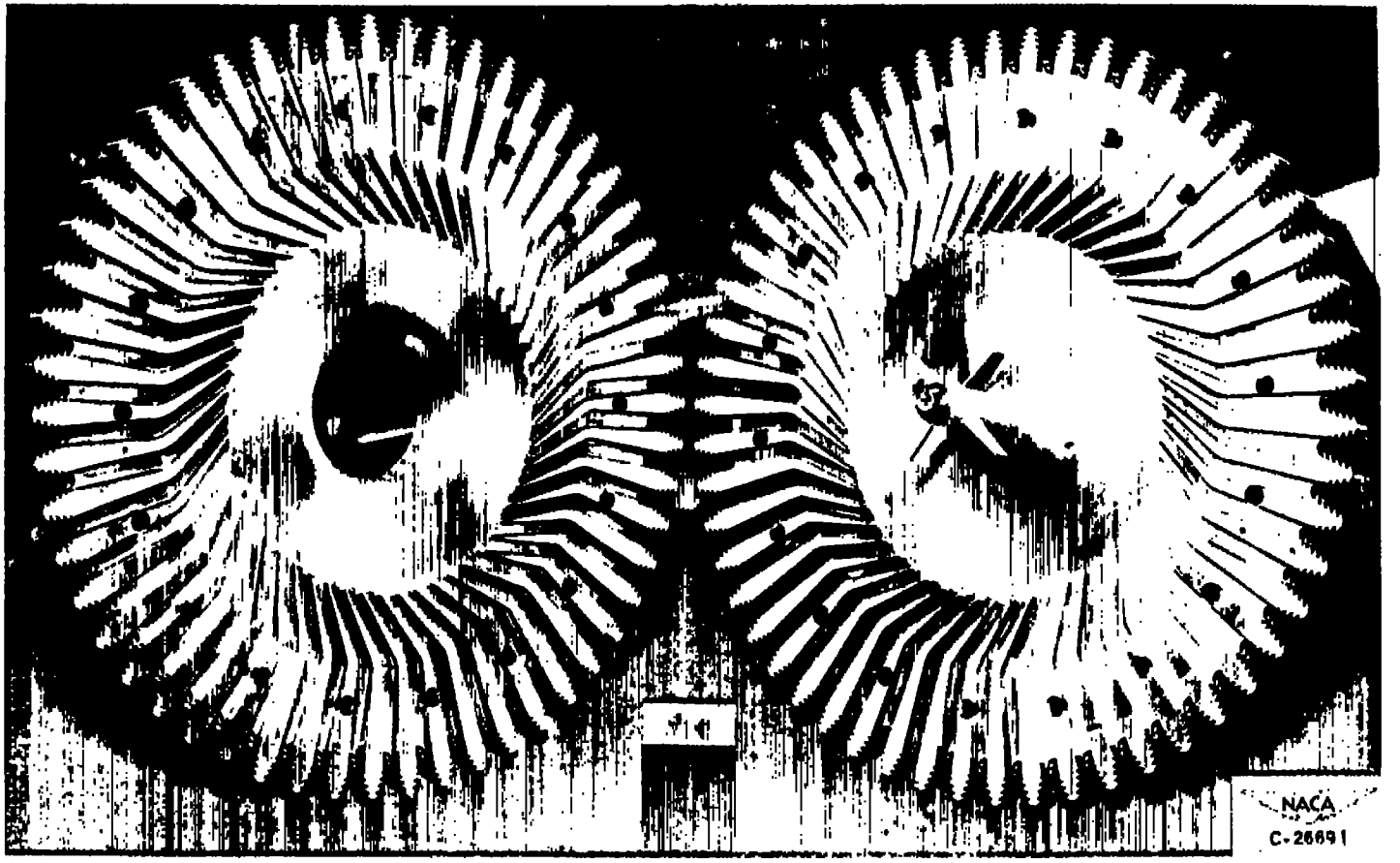

Rear disk Forward disk

Figure 2. - Internal cooling-air impeller vanes in both halves of wheel; spider shown on forward disk.

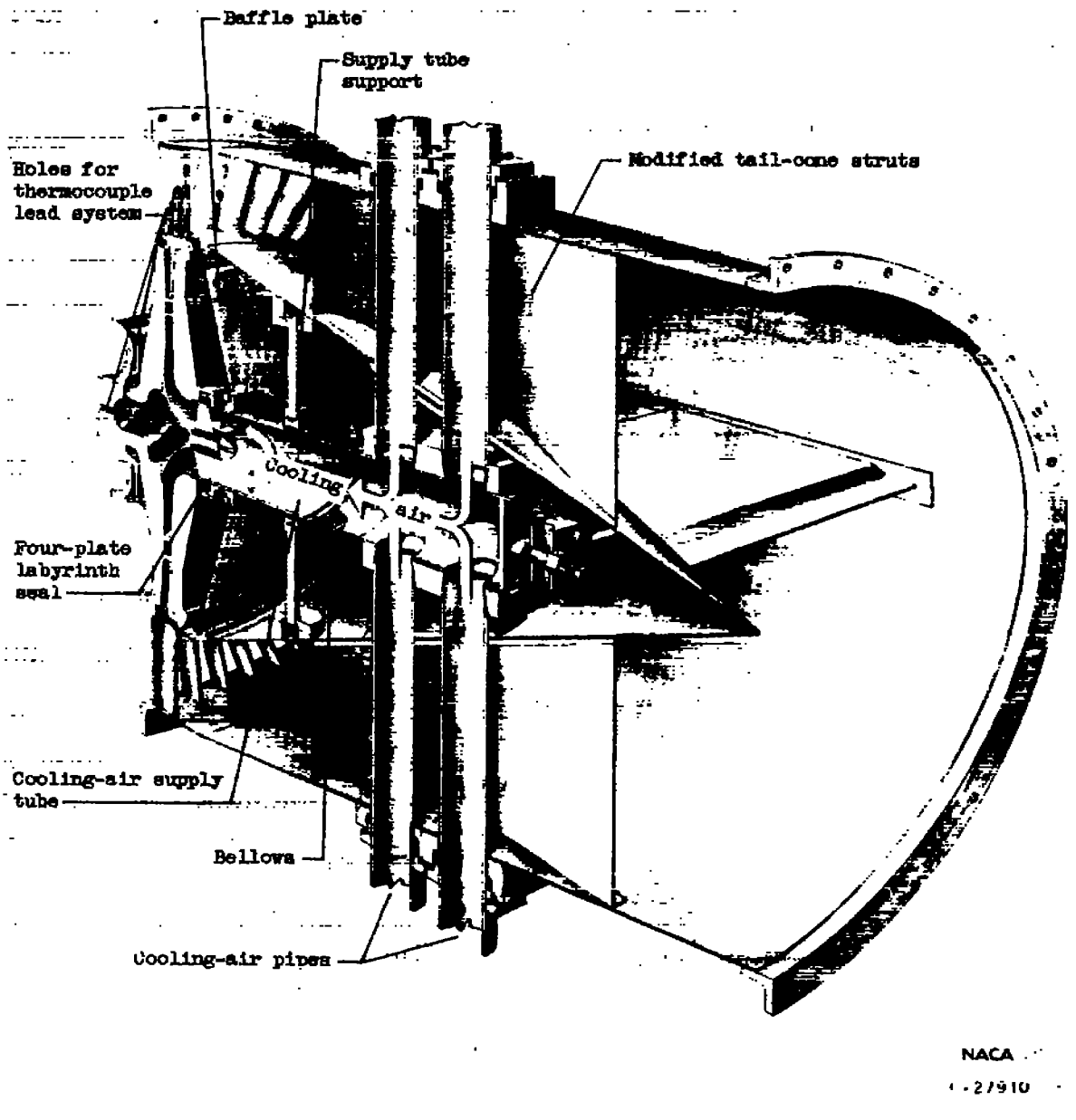

Figure 3. - Tail-cone modifications for introduction of cooling air.

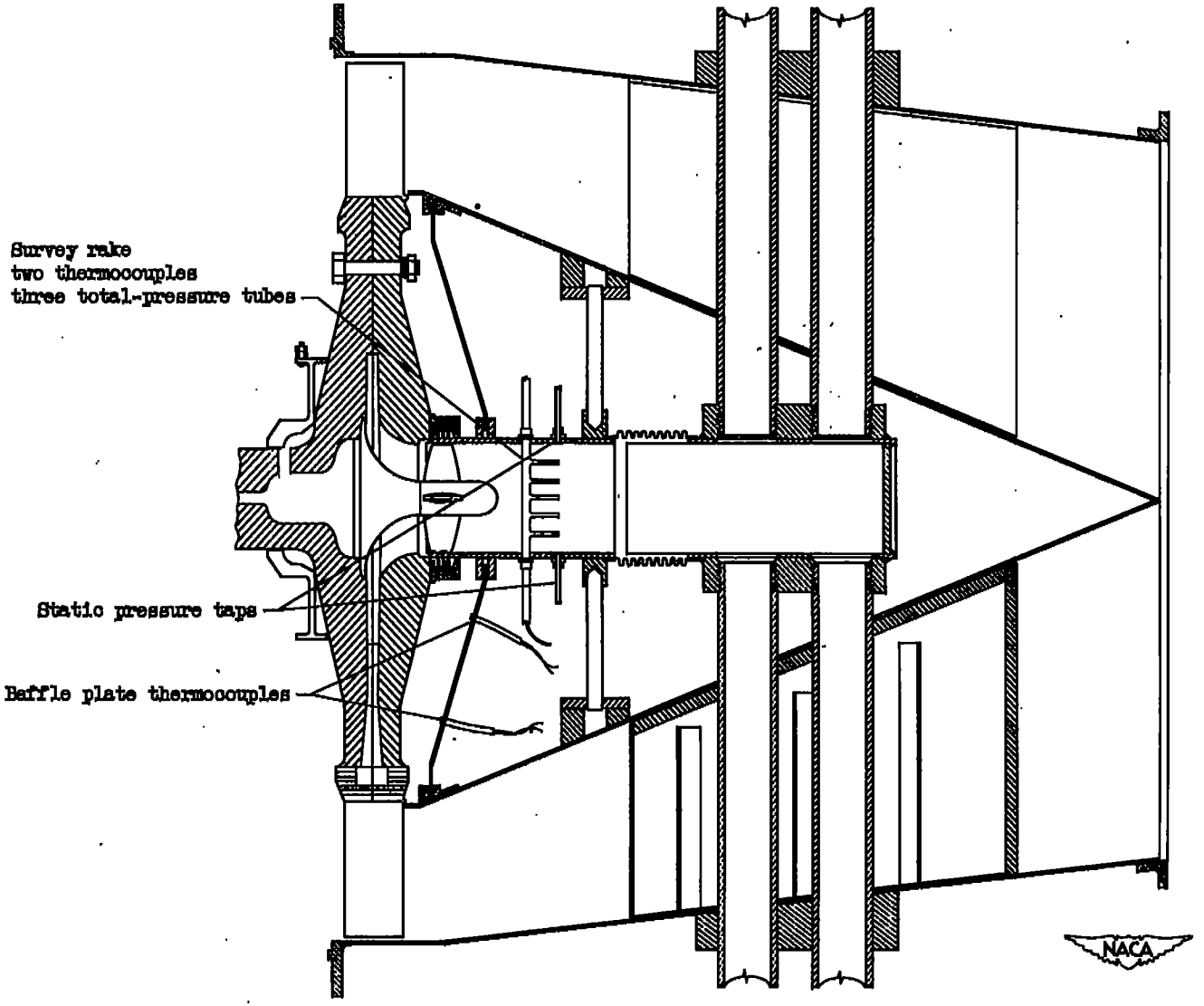

Figure 4. - Instrumentation in modified tail cone.

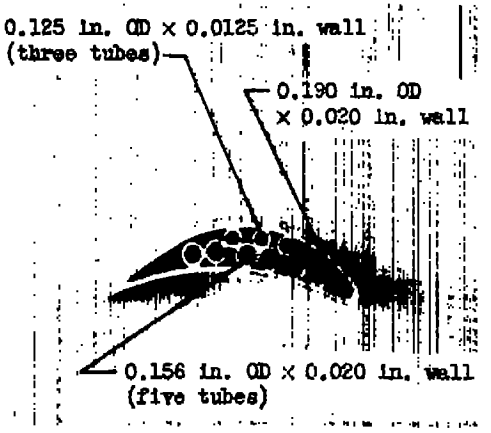

(a) Tip profile showing tube arrangement and size.

(b) Coolant passage entrance in base.

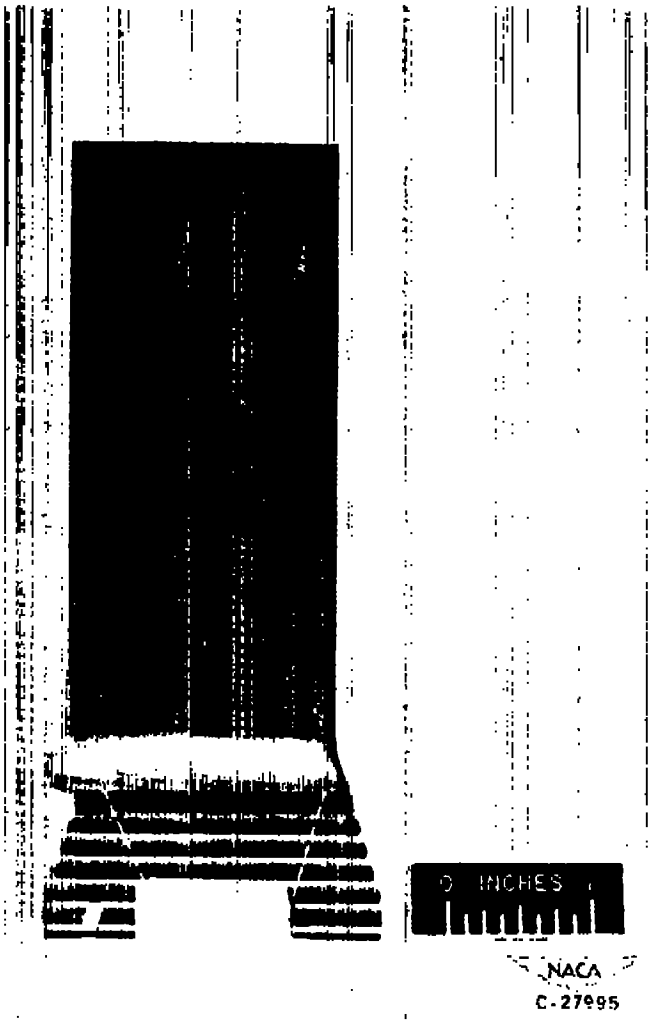

(c) Side view.

Figure 5. - Cast X-40 alloy air-cooled blade with nine-tube insert from J33 turbine rotor.

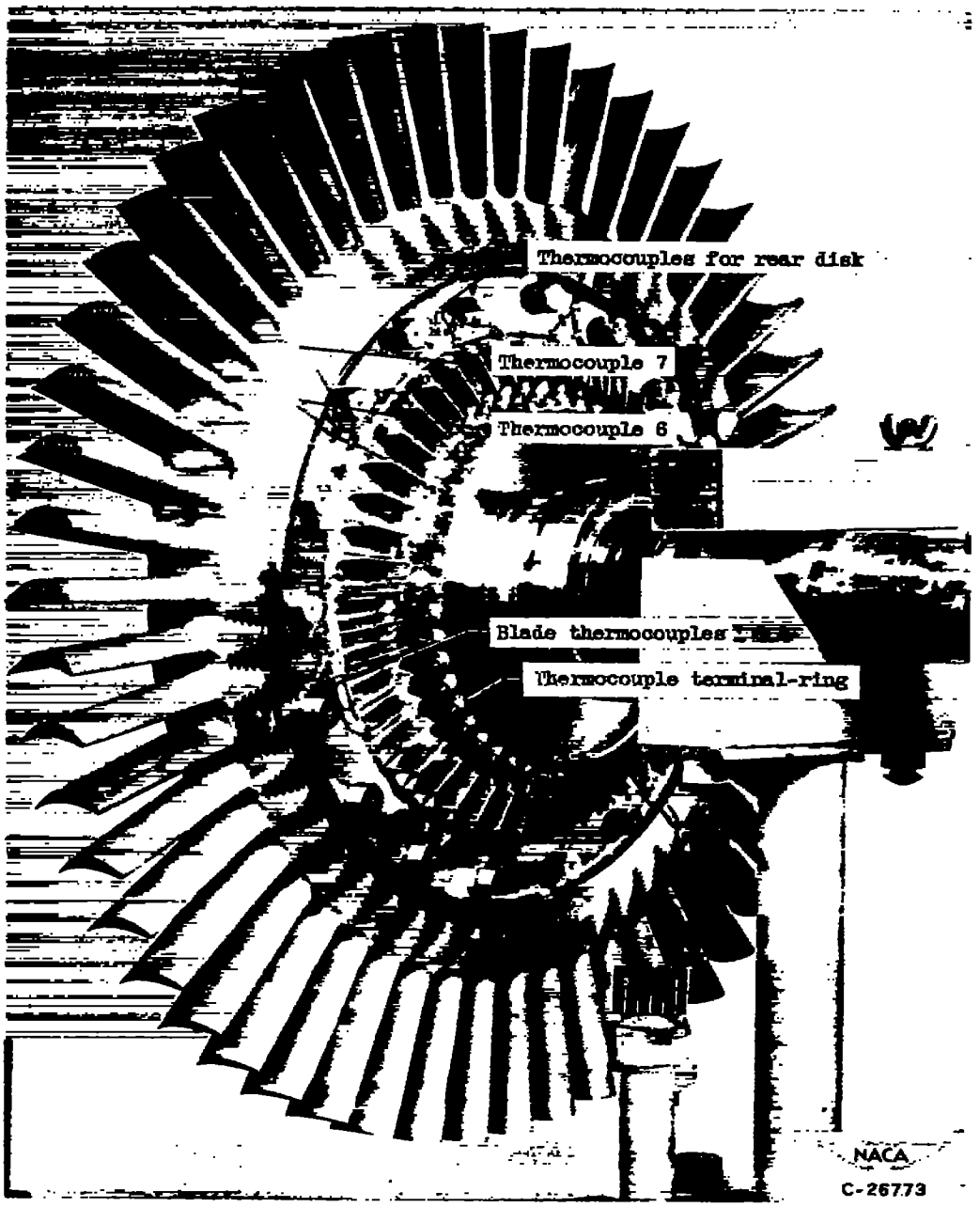

Figure 6. - Modified J33 air-cooled turbine rotor showing thermocouple installation.

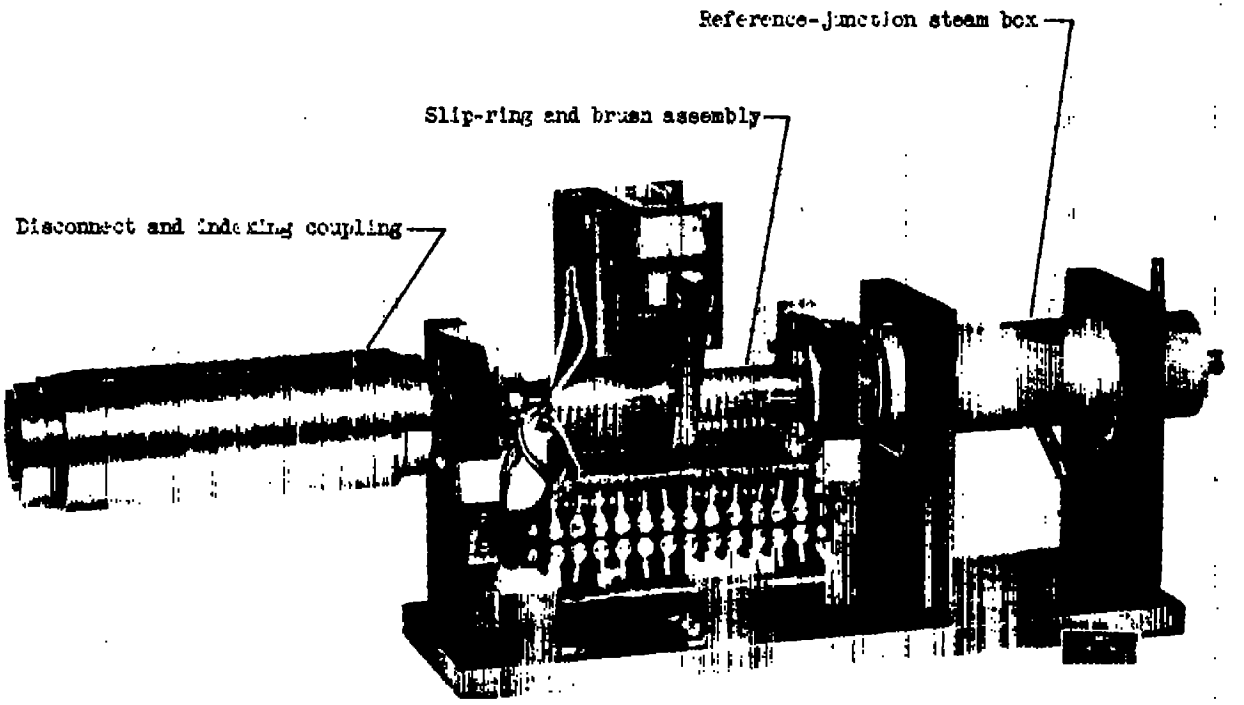

Figure 7. - Thermocouple slip-ring assembly with indexing coupling attached.

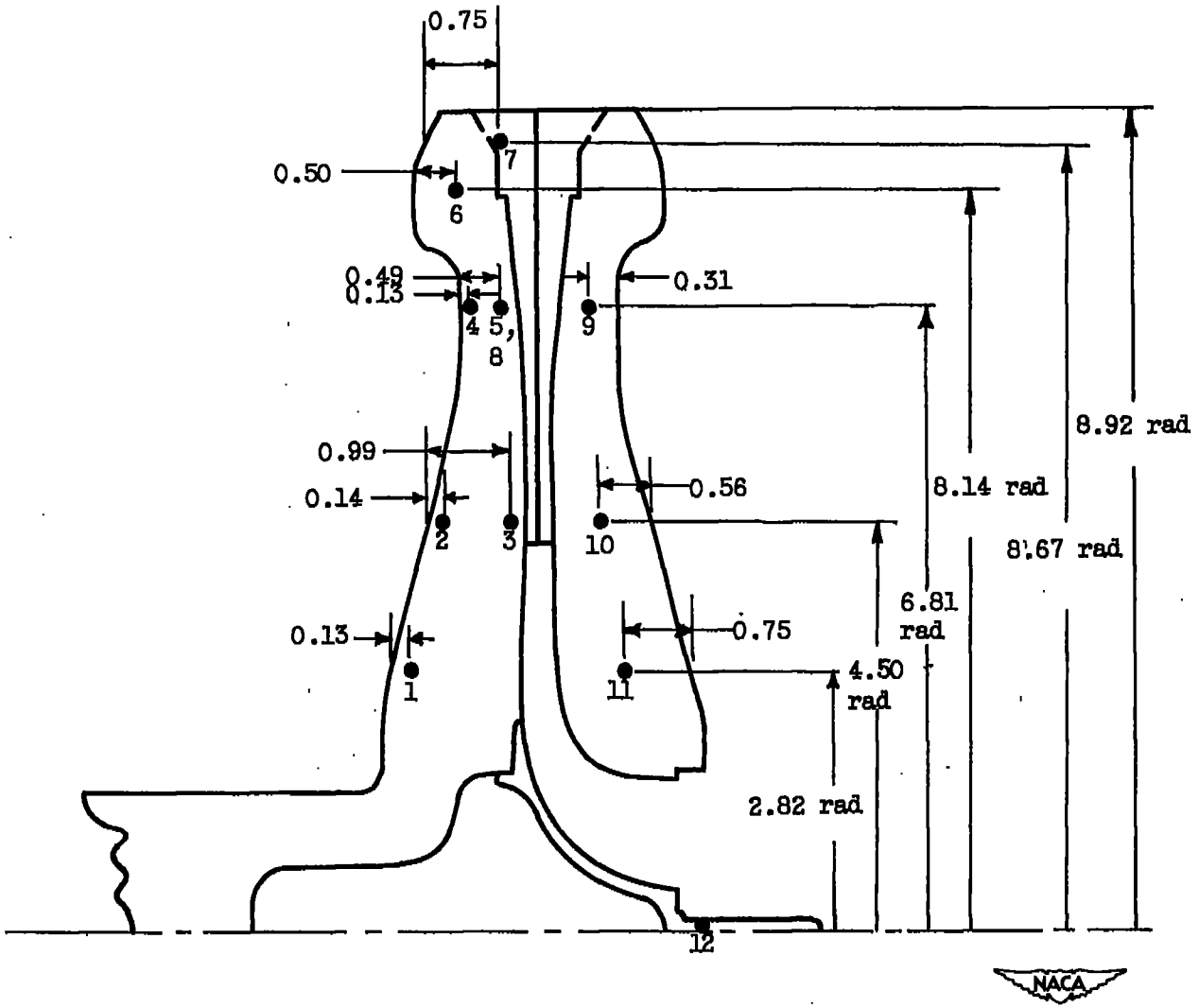

Figure 8. - Turbine disk thermocouple locations. (All dimensions in inches.)

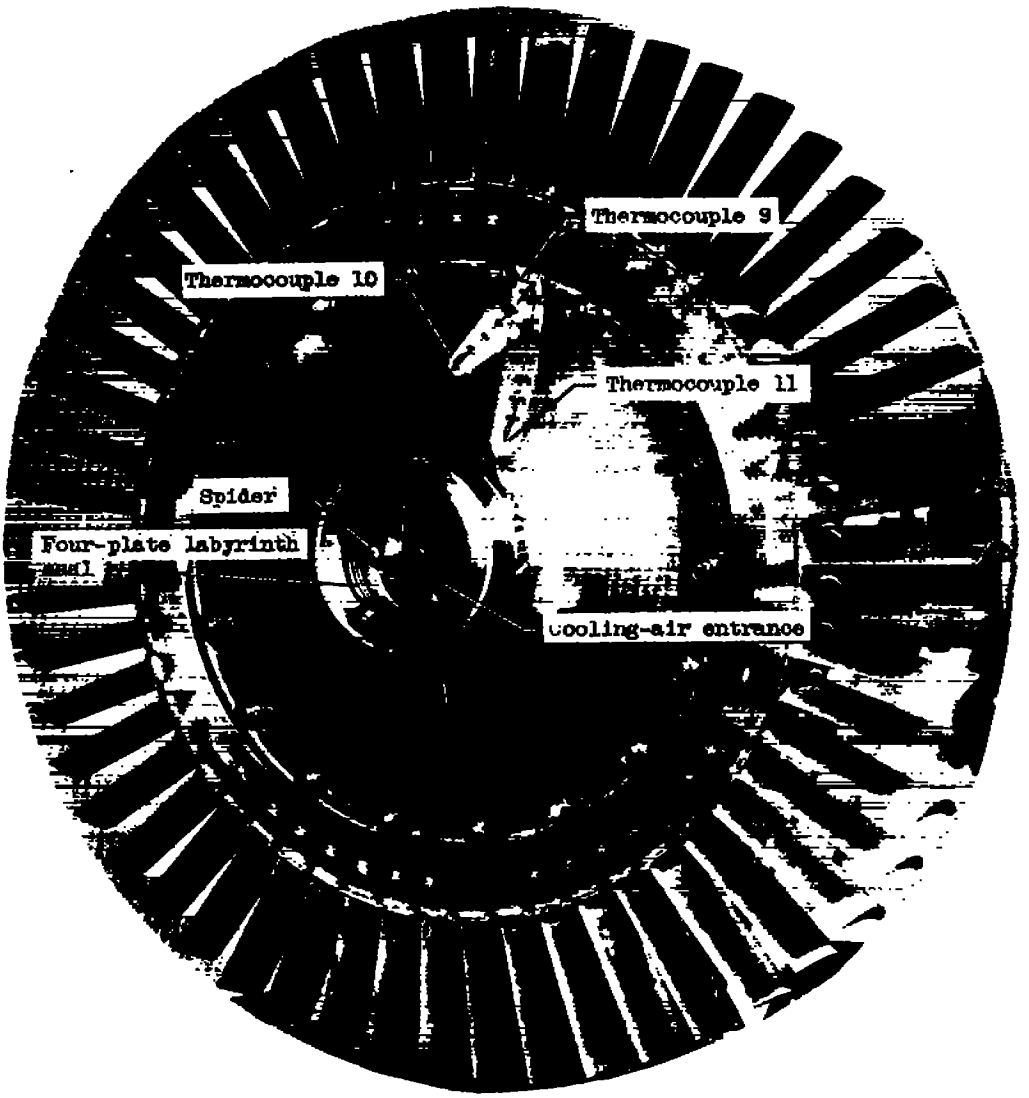

Figure 9. - Modified J33 air-cooled turbine rotor showing thermocouple installation in rear disk.

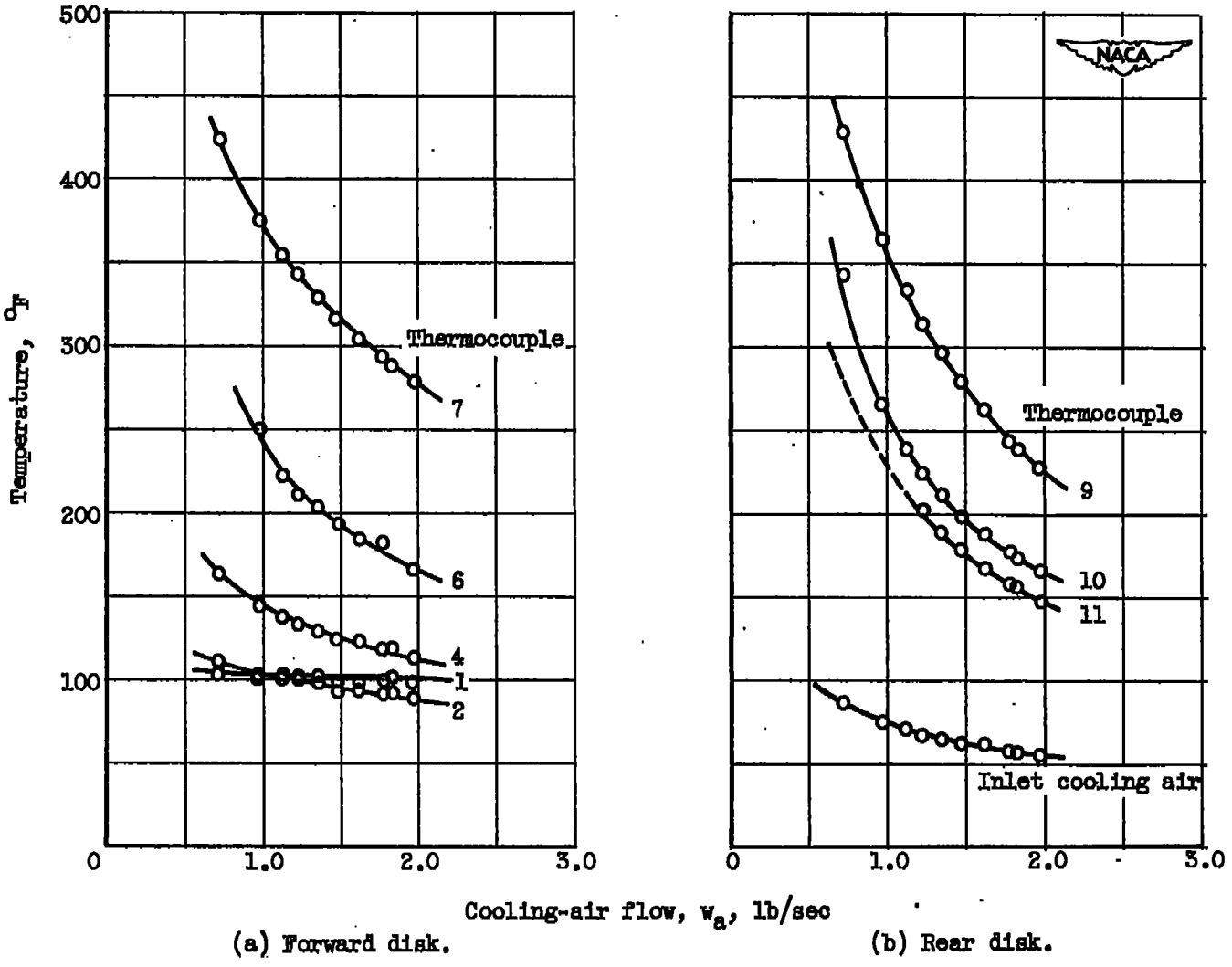

Figure 10. - Variation of disk temperatures and cooling-air temperature with cooling-air flow at engine speed of 4000 rpm; average effective gas temperature, 1152° F.

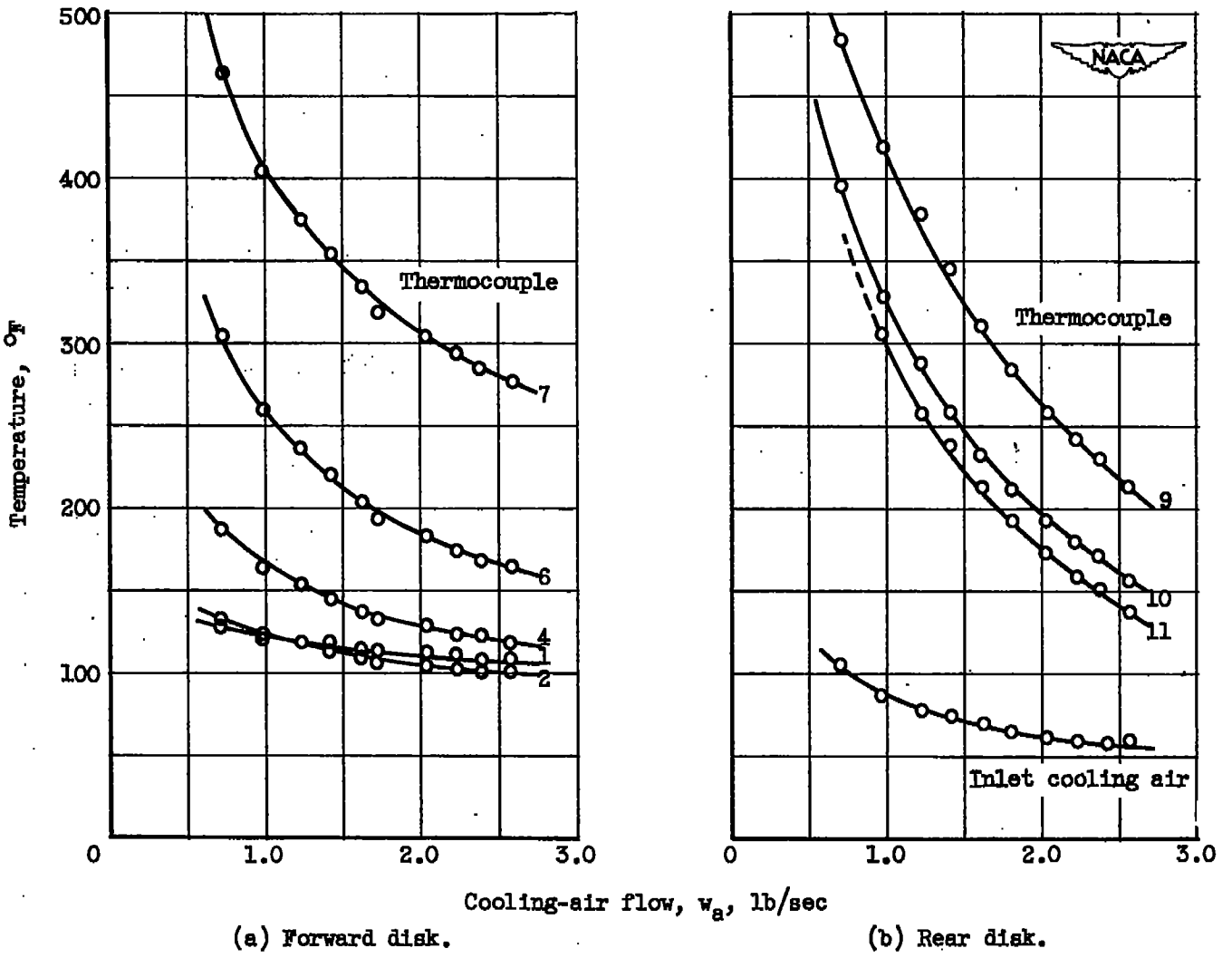

Figure 11. - Variation of disk temperatures and cooling-air temperature with cooling-air flow at engine speed of 5000 rpm; average effective gas temperature, 1170° F.

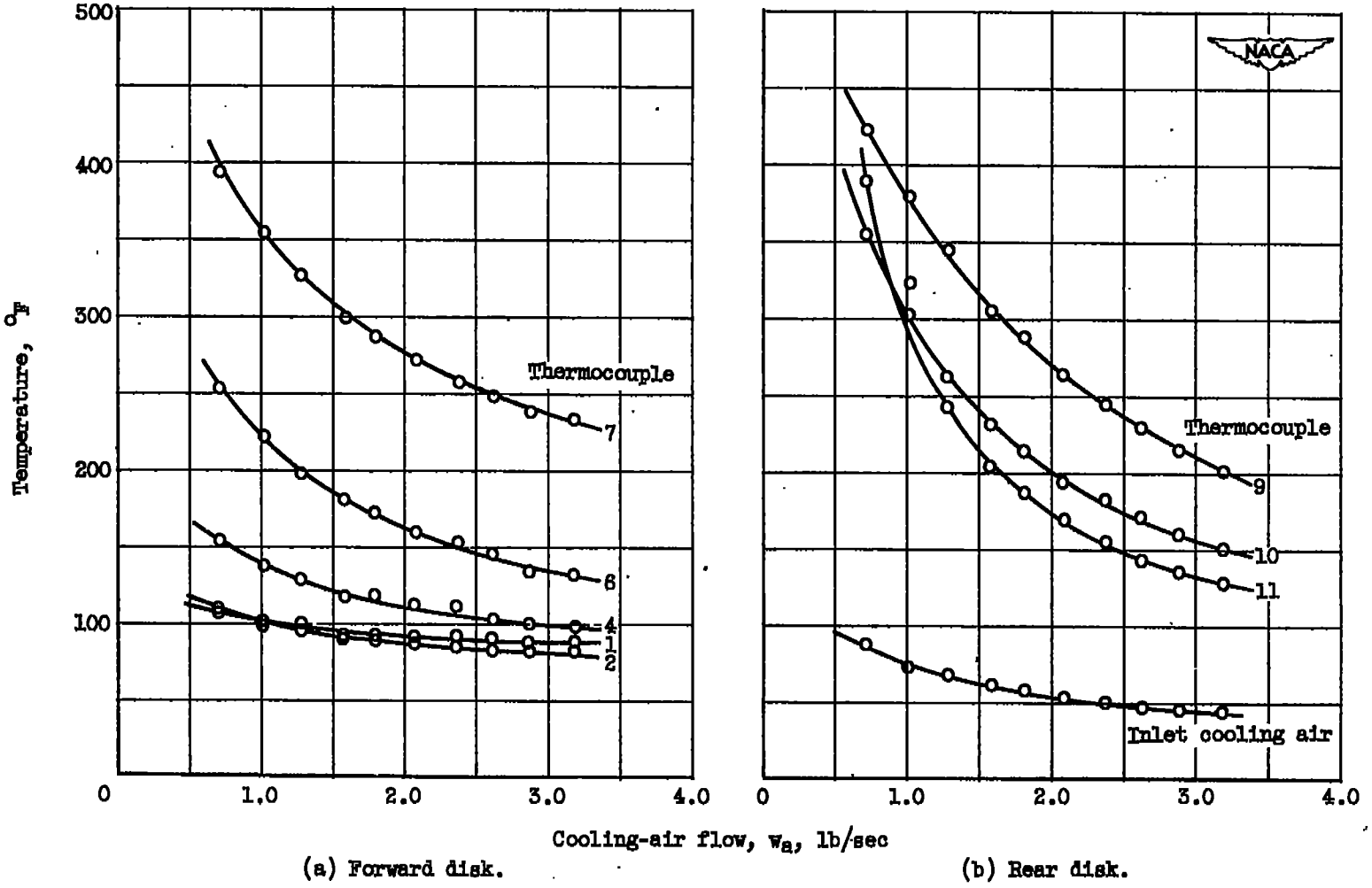

Figure 12. - Variation of disk temperatures and cooling-air temperature with cooling-air flow at engine speed of 6000 rpm; average effective gas temperature, 1039° F.

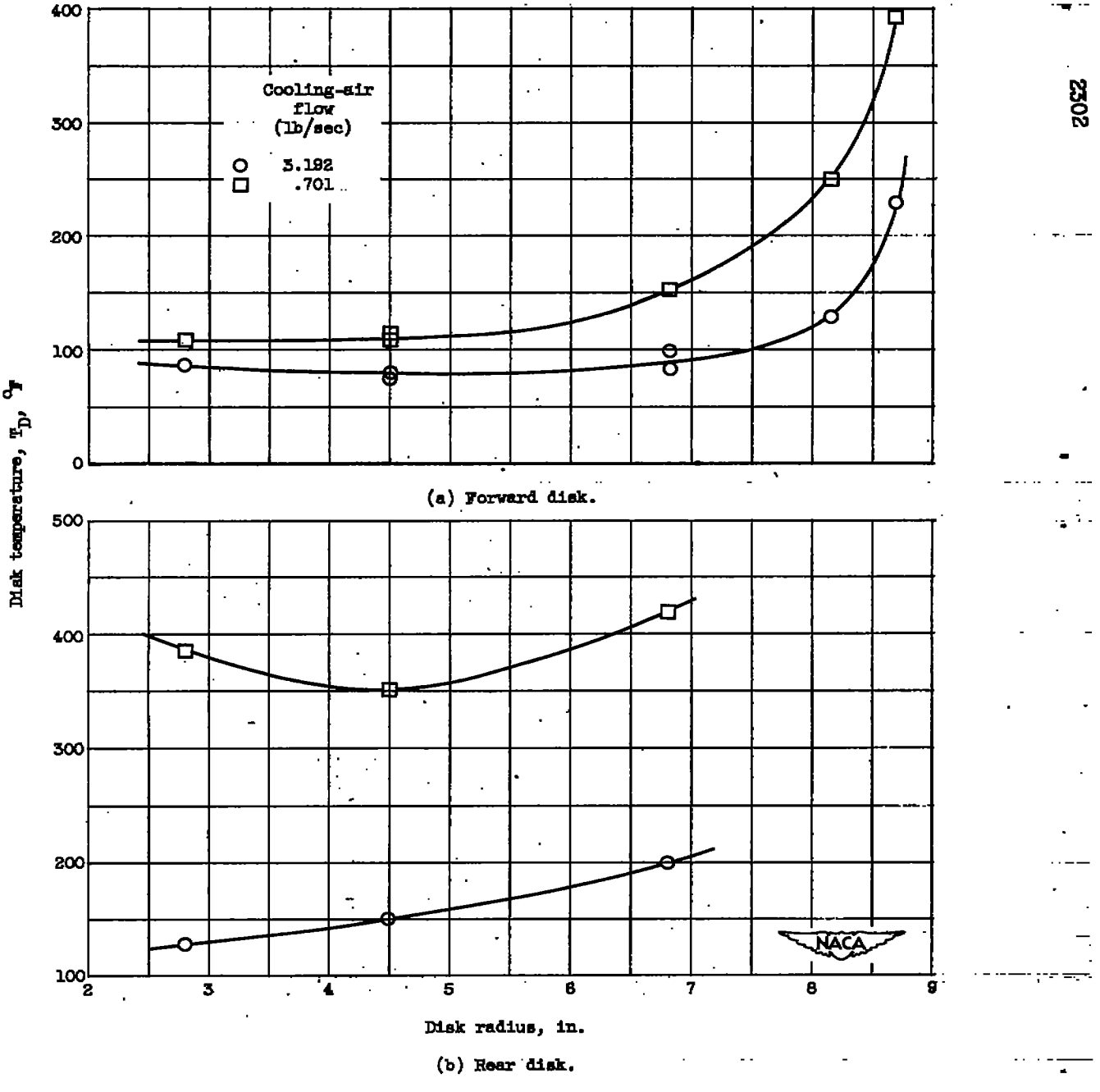

(b) Rear disk.

Figure 13. - Radial disk temperature distribution for two cooling-air flows. Engine speed, 6000 rpm; average combustion-gas flow, 33.5 pounds per second; average effective gas temperature, 1039° F.

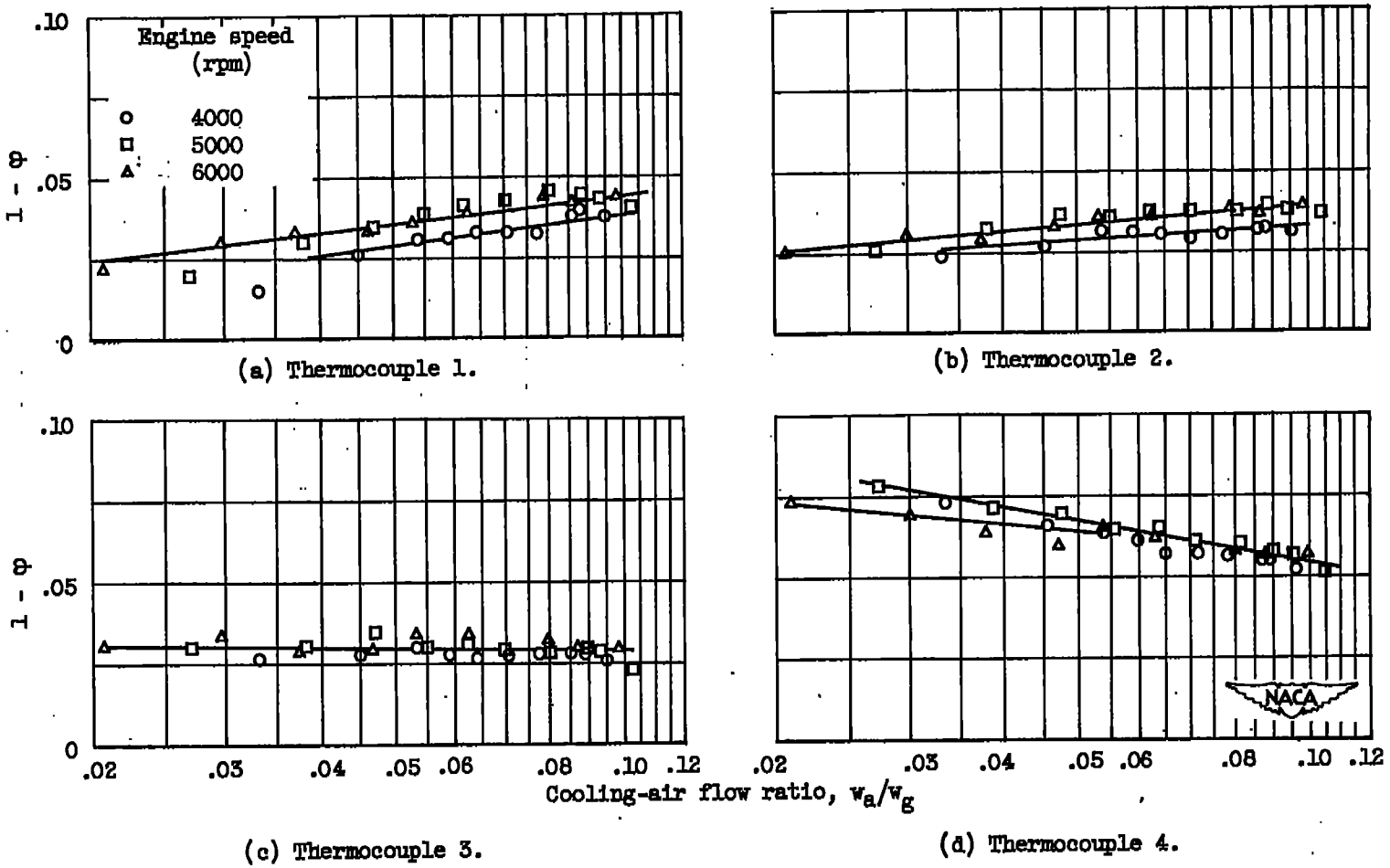

(a) Thermocouple 1.

(b) Thermocouple 2.

(c) Thermocouple 3.

(d) Thermocouple 4.

Figure 14. - Correlation of disk temperatures with cooling-air flow ratio at several engine speeds.

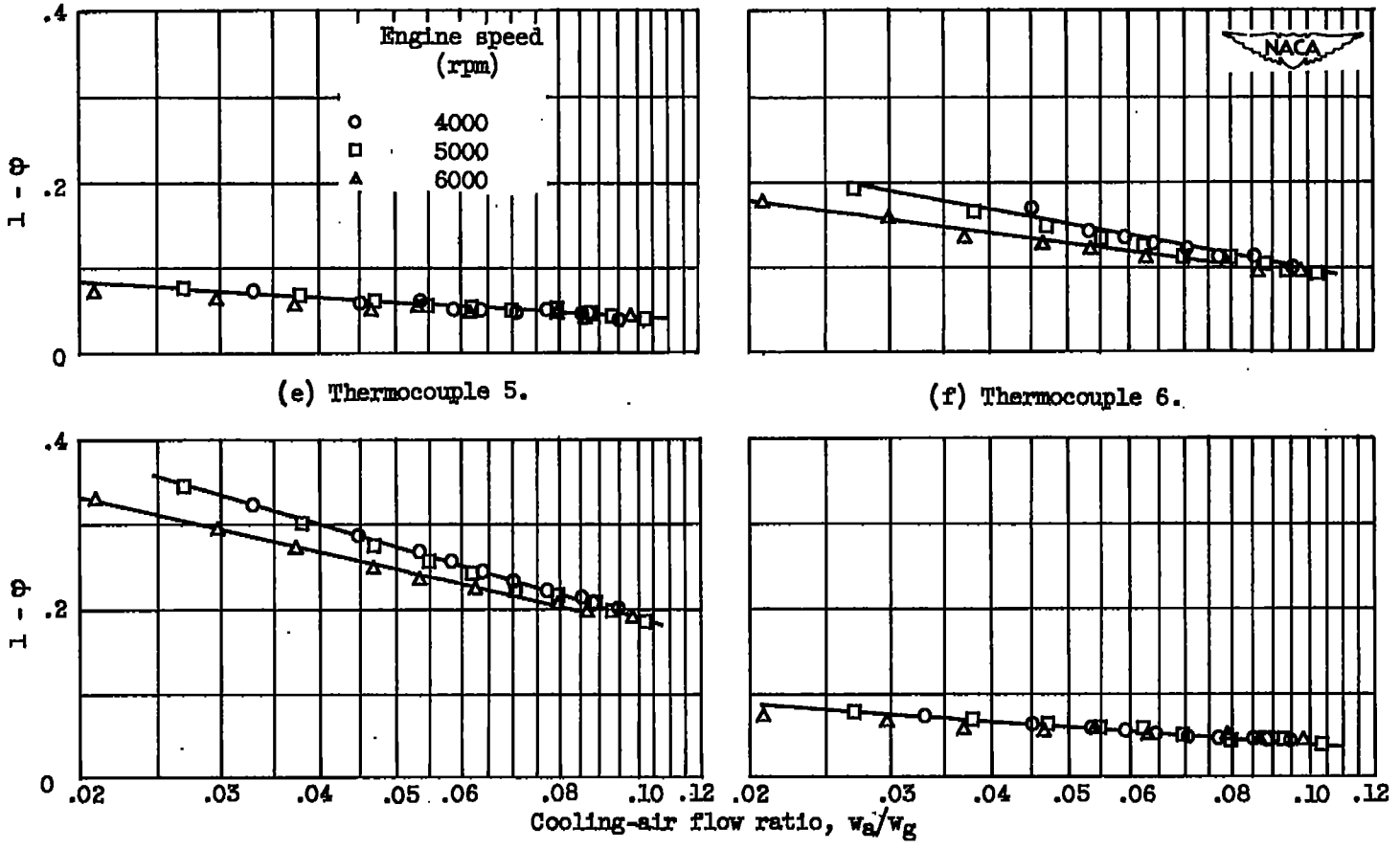

(e) Thermocouple 5.

(f) Thermocouple 6.

(g) Thermocouple 7.

(h) Thermocouple 8.

Figure 14. - Continued. Correlation of disk temperatures with cooling-air flow ratio at several engine speeds.

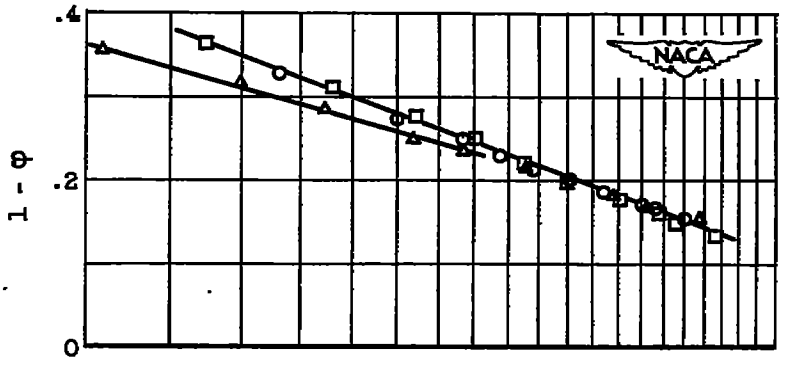

(i) Thermocouple 9.

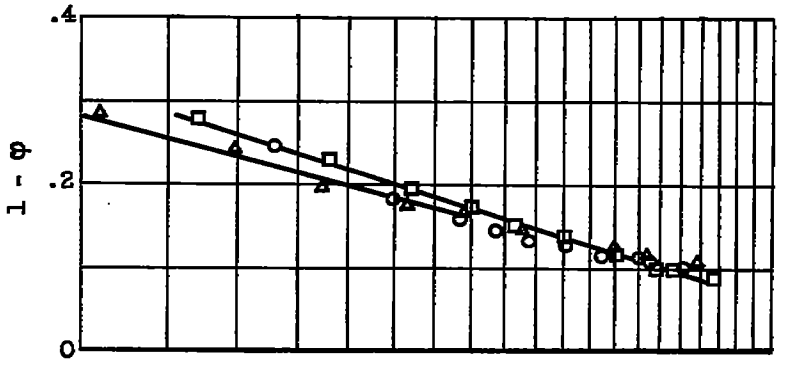

(j) Thermocouple 10.

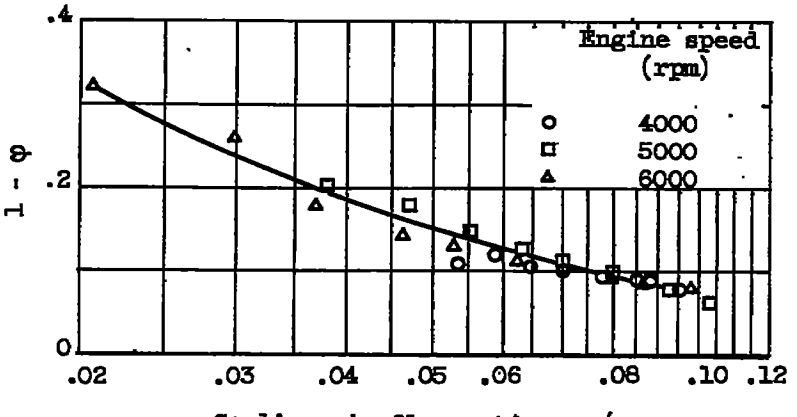

(k) Thermocouple 11.

Figure 14. - Concluded. Correlation of disk temperatures with cooling-air flow ratio at several engine speeds.

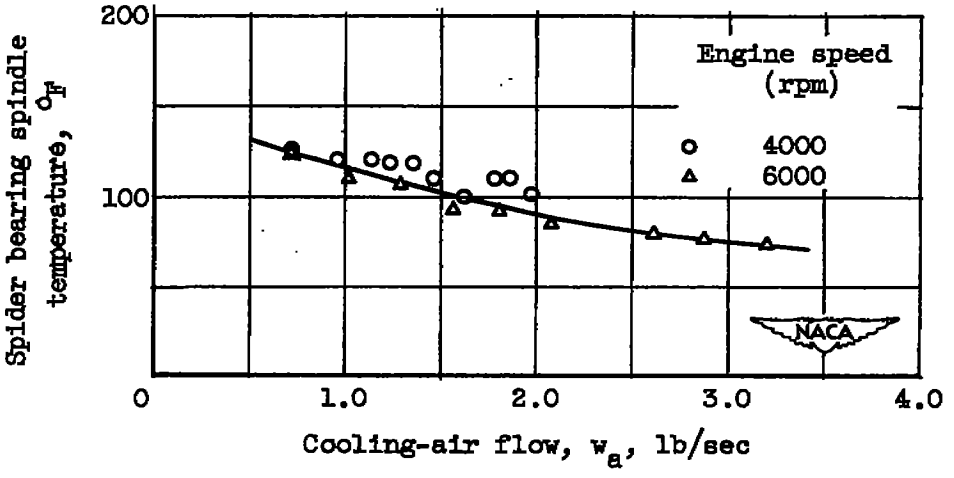

Figure 15. - Variation of spider bearing spindle temperature with cooling-air flow for two engine speeds.

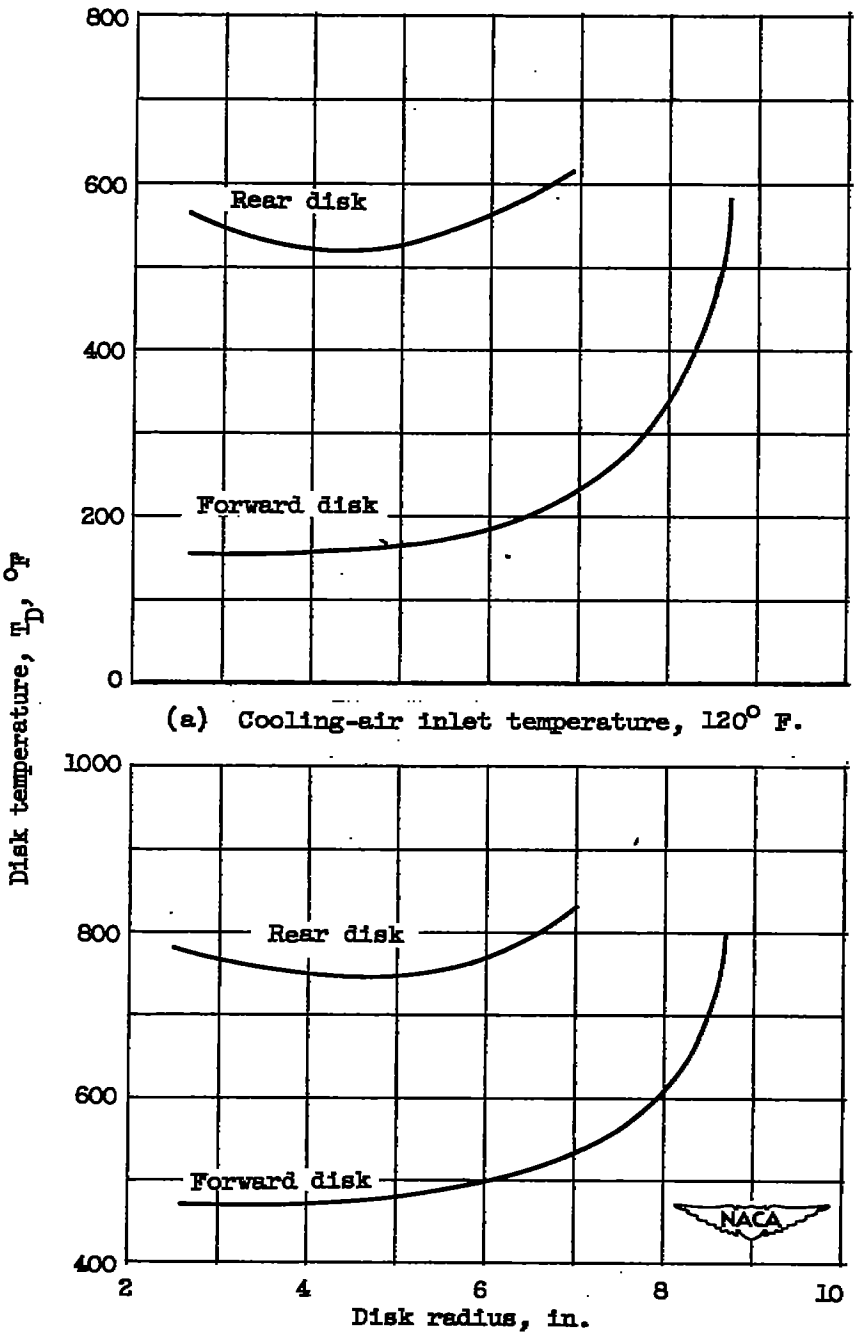

(a) Cooling-air inlet temperature, 120° F.

(b) Cooling-air inlet temperature, 445° F.

Figure 16. - Calculated disk temperatures for modified J33 engine. Engine speed (rated), 11,500 rpm; cooling-air flow ratio, 0.02; average effective gas temperature, 1445° F.

[redacted]